Nuclear Inst. and Methods in Physics Research B 455 (2019) 140–145

Contents lists available at ScienceDirect

Nuclear Inst. and Methods in Physics Research B

journal homepage: www.elsevier.com/locate/nimb

Groundwater flow traced by bomb pulses of ^{36}Cl and tritiogenic ^{3}He in a borehole

Yasunori Mahara[a,*], Tomoko Ohta[b]

[a] Kyoto University, Kyoto, Kyoto 606-8501, Japan
[b] Department of Environmental Systems, School of Frontier Science, The University of Tokyo, Kashiwa-shi, Chiba 277-8563, Japan

ARTICLE INFO

Keywords:
Global fallout
Bomb pulse
^{36}Cl
^{3}H
Tri^{3}He
Piston flow

ABSTRACT

In 2001, a borehole was drilled to 400 m depth below the ground surface of a tableland in northern Japan, where horizontal porous sedimentary rock strata are deposited. Fresh drill-core and groundwater samples were collected from the borehole for estimating global fallout bomb pulses of ^{3}H, which becomes tritiogenic ^{3}He (tri^{3}He) through β-decay, and ^{36}Cl. In the northern hemisphere, the maximum fallout deposition of ^{36}Cl from nuclear testing was observed during 1954–1957, and that of ^{3}H in 1963. Most ^{3}H (half-life 12.3 y) in the rock porewater had decayed to tri^{3}He during the 38 years between 1963 and 2001. In the borehole, bomb pulses were observed in profiles of tri^{3}He and ^{36}Cl/Cl at 101 m and around 138 m depth below the ground surface, respectively. The downward groundwater velocity was estimated to be 2.9–3.1 m/y from the depth of the ^{36}Cl/Cl bomb pulse and 2.7 m/y from the depth of the tri^{3}He bomb pulse. Although the two velocity estimates differ by 10–15%, it is possible to model groundwater flow in the tableland as downward piston flow without diffusion.

1. Introduction

Many groundwater surveys (e.g. [1]) conducted for the last several decades have examined local groundwater flow on the tableland in northern Japan and its interaction with the regional groundwater flow. These hydrogeological surveys used various environmental tracers to trace groundwater flow, and some studies combined analyses of radionuclides with long and short half-lives to estimate the origin of the groundwater and its circulation pattern. Radioactive environmental tracers (here ^{3}H and ^{36}Cl) are naturally produced by interactions of cosmic rays with the air or surface rocks, or by in situ neutron activation in deep rock. The major target elements for ^{3}H production are N, O, and Li, and those for ^{36}Cl are Ar, K, Ca, and Cl. On the other hand, many of these radionuclides were globally released to the environment by thermonuclear testing in the 1950 s and 1960 s and, unfortunately, by nuclear facilities as well, either accidentally or operationally [2–5].

Global fallout bomb pulses of ^{36}Cl and ^{3}H were observed in precipitation in the northern hemisphere in the mid-1950 s [2] and in 1963 [6], respectively. Because the half-life of ^{36}Cl (3×10^{5} y) is much longer than that of ^{3}H (12.3 y), the loss of ^{36}Cl due to decay was negligibly small at the time of the 2001 hydrogeological survey of the tableland. In contrast, most ^{3}H in rock porewater and groundwater had decayed to tritiogenic ^{3}He (tri^{3}He) during the 38 years or more since rainwater containing the bomb pulse had begun to gradually infiltrate the tableland. In this study, we estimated the origin, residence time, and local downward flow velocity of groundwater in the tableland by using ^{36}Cl and ^{3}H (i.e., tri^{3}He) as environmental tracers.

2. Geological setting of the site

Concentrations of ^{3}H and ^{36}Cl from global fallout were measured in rock porewater and groundwater samples collected in 2001 from a newly drilled borehole on the Pacific side of northern Japan (Fig. 1). The sampling site is near a shallow, brackish lake on a tableland where the maximum elevation is 50 m above sea level. At the site, Quaternary strata deposited during the past 400 ky overlie a thick sequence of Tertiary rocks deposited before 5 Ma and consisting of tuffaceous sandstone (hydraulic conductivity around 10^{-7} to 10^{-10} m/s), coarse and fine sandstone (hydraulic conductivity around 10^{-8} to 10^{-10} m/s), and mudstone (hydraulic conductivity around 10^{-9} to 10^{-10} m/s) [1] (Fig. 1). Because the mudstone has low permeability and underlies the area around the borehole site (the top surface of the mudstone is 268 m below ground level), it controls the regional groundwater flow. The studied borehole was drilled near the southeastern margin of the tableland. The top of the borehole (ground level) is at 32.3 m above sea level, and the bottom of the borehole is at −390 m relative to ground level. Hereafter, all depths are expressed relative to ground level.

Climate and hydrological conditions was reported as follows [1].

* Corresponding author.
E-mail address: mahara.yasunori.u40@kyoto-u.jp (Y. Mahara).

https://doi.org/10.1016/j.nimb.2018.12.023
Received 22 November 2017; Received in revised form 6 June 2018; Accepted 10 December 2018
Available online 23 December 2018
0168-583X/ © 2018 Elsevier B.V. All rights reserved.

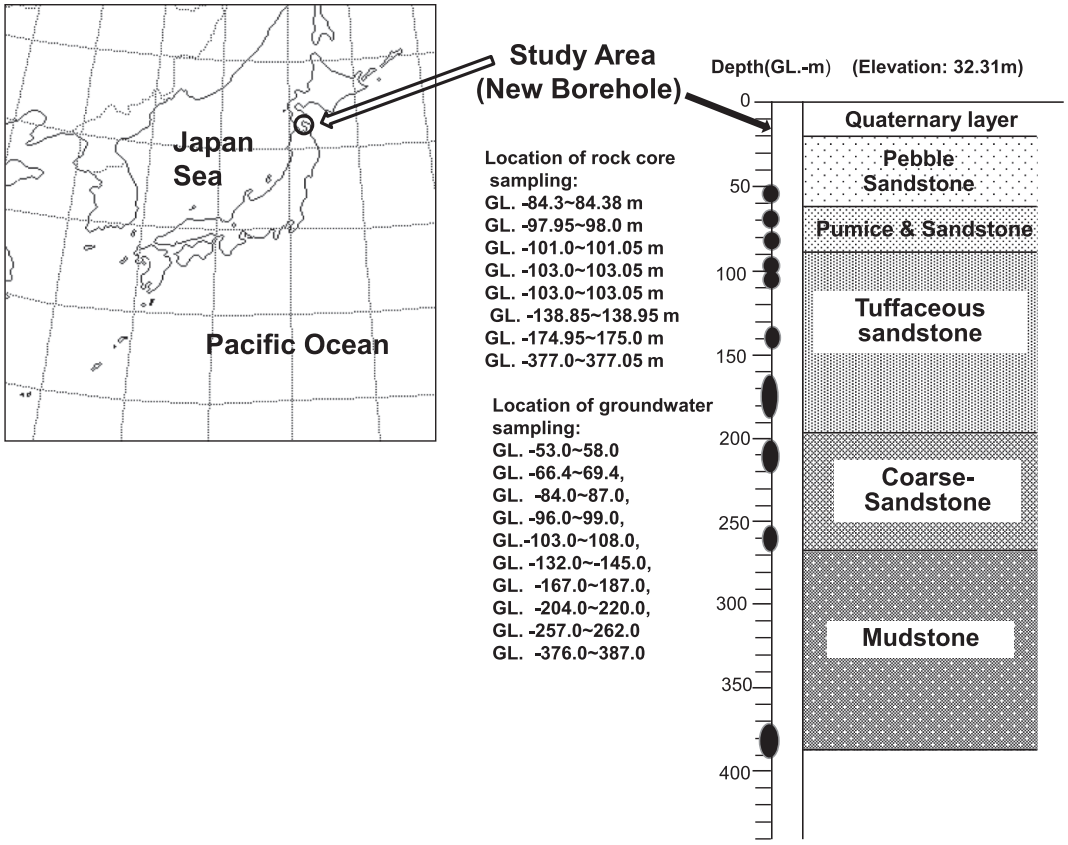


Fig. 1. study area in the northern Japan (location of the new borehole and vertical geological formations, Solid black circle: core and groundwater sampling location in borehole).

Average annual air temperature and precipitation at the site were 8 °C and 1065 mm, respectively. Snow covered the ground for about four months of the year. The average evapotranspiration rate estimated by the method of Penman [7] was 400 mm/y, and the average surface runoff was empirically found to be 365 mm/y. Therefore, the net rate of recharge by precipitation of the tertiary sedimentary strata can be estimated to be 300 mm/y.

3. Materials and methods

3.1. Groundwater and soil water sampling

After drilling was completed, 10 groundwater samples were collected from the borehole at the depth intervals indicated in Fig. 1 with a sampling device that uses a water-inflatable packer system to prevent mixing of water from different sections of the borehole. Groundwater samples (2.02 L each) for measuring ^{36}Cl, stable isotopes, and dissolved ions were collected in two 1-L plastic bottles and two 10-mL glass vials, after first pumping out of the borehole three times the volume of the isolated section to exchange stagnant water in the section with fresh rock formation water.

Soil water samples consisting of the free water component ($< p$F 3) [7], that is, water flowing under gravity, were collected from 25-cm-long unsaturated soil cores by a centrifugation method.

3.2. Rock porewater sampling

During the drilling of the borehole, seven fresh rock cores were collected from five geological strata at the depth intervals shown in Fig. 1 for measurement of ^{4}He and ^{3}He dissolved in porewater in the rock. Rock core samples (each trimmed to a diameter of 40 mm and a length of 50–100 mm) were cut from each core section immediately after it was lifted to the ground surface for measurement of noble gas concentrations in the porewater. To avoid atmospheric air contamination, the surface of each rock sample was flushed with nitrogen gas and the samples were tightly sealed in stainless steel containers that had been evacuated of residual gases for 1–2 min via pumping through an annealed copper tube welded to the container top; the tube was pinched off with a steel clamp [8]. Each rock core container was stored in a water pool for approximately 3 months to allow the dissolved gases in the porewater to diffuse until their concentrations were in equilibrium throughout the container. The intrusion rate of atmospheric ^{4}He into the container was less than 1.73×10^{-12} cc (STP)/day during storage.

3.3. Analytical methods

Dissolved chloride ions were precipitated as AgCl from each sample solution in a clean ventilation draft system equipped with a clean bench. The precipitate was purified by repeated dissolution in NH_4OH, sulfur removal as $BaSO_4$, and reprecipitation. Then, ^{36}Cl/Cl ratios were measured by accelerator mass spectrometry at Australian National University. The ^{36}Cl/Cl ratio of a blank sample was $(0.04 \pm 0.04) \times 10^{-15}$ [9], and the measurement error was less than 30% around the lower ratio of 10^{-15} [10,11].

For measurement of ^{4}He, moisture and active gases were first removed from each sample by a cold trap and a heated getter pump, then each noble gas component was separated by cooling the sample in a charcoal trap with liquid nitrogen by using a cryogenic pump, following the procedure described in detail by Nagao et al. [12]. Then, a VG-5400 noble gas mass spectrometer was used to measure the dissolved noble gas concentrations and their isotopic ratios.

For estimation of the origin of the soil water and groundwater, the stable isotopes δD and δ^{18}O were measured by mass spectrometry after reducing the water in the sample to H_2 and after the water and gaseous

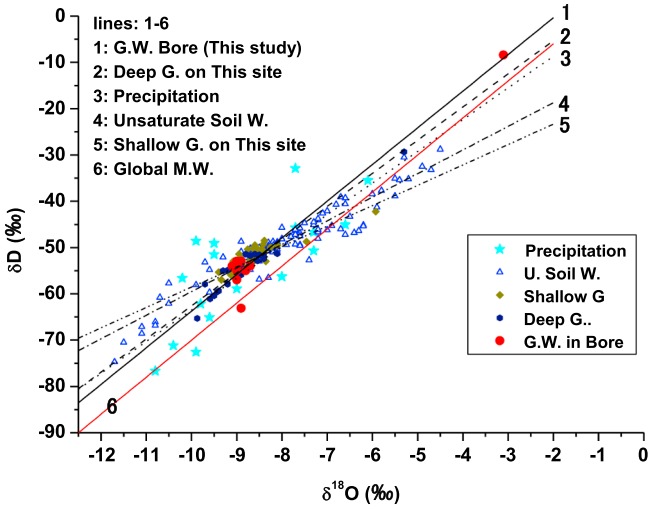


Fig. 2. Stable isotopes correlation between δD and $\delta^{18}O$ (Precipitation, Soil water, Shallow groundwater, Deep groundwater, and Groundwater in new borehole).

CO_2 has reached isotopic equilibrium. Both δD and $\delta^{18}O$ were expressed as per mil (‰) deviations from Vienna Standard Mean Ocean Water (VSMOW). The measurement error was ± 1‰ for δD and ± 0.1‰ for $\delta^{18}O$.

4. Results and discussion

4.1. Origins of the soil water and groundwater

Regression was used to compare the δD vs. $\delta^{18}O$ relationships of five data sets to the global meteoric water line ($\delta D = 8.0 \times \delta^{18}O + 10$) as follows (Fig. 2): precipitation at the borehole site ($\delta D = 6.60 \times \delta^{18}O + 3.67$; $n = 18$, $r^2 = 0.60$), unsaturated soil water ($\delta D = 5.10 \times \delta^{18}O - 8.49$; $n = 114$, $r^2 = 0.90$), shallow ($\delta D = 4.38 \times \delta^{18}O - 14.6$; $n = 55$, $r^2 = 0.78$) and deep groundwater ($\delta D = 7.16 \times \delta^{18}O + 9.02$; $n = 26$, $r^2 = 0.93$), and groundwater samples collected from the newly drilled borehole ($\delta D = 7.92 \times \delta^{18}O + 15.47$; $n = 10$, $r^2 = 0.96$). Interestingly, total annual precipitation could be separated into summer (April–September: $\delta D = 8.0 \times \delta^{18}O + 10.1$; $n = 10$, $r^2 = 0.97$) and winter (October–March: $\delta D = 6.71 \times \delta^{18}O + 11.42$; $n = 8$, $r^2 = 0.57$) precipitation. This result reflects the fact that precipitation on the tableland is controlled by moisture in Pacific air masses during the summer and by moisture from the Japan Sea taken up by cold, dry air masses from the Asian continent during the winter [13]. Furthermore, the stable isotopic composition of the waters gradually changed as a result of evapotranspiration as water infiltrated through the unsaturated soil layer toward the water table. In the shallow groundwater environment, the stable isotope ratios reflect the mixing of soil waters that had followed different flow paths. The stable isotope ratios in deep groundwater may reflect the local characteristics of the tableland and the mixing of shallow groundwaters (that had followed different flow paths) with deeper groundwater masses differing with respect to their size and residence time. The $\delta D/\delta^{18}O$ ratio of groundwater should be roughly 8.0 if it originated as meteoric water [14]. Therefore, we inferred that the water samples collected from the drilled borehole originated mainly from meteoric water.

4.2. Maximum depositions of ^3H and ^{36}Cl from global fallout at the borehole site

To determine the timing of maximum radionuclide deposition at the studied site, we compared ^{36}Cl deposition recorded in Arctic ice cores and ^3H in precipitation to known releases during global nuclear weapons testing (Fig. 3). We calculated the global deposition of ^3H from concentrations in precipitation observed in middle latitudes, namely, at Ottawa, Canada (45.32° N, 75.67° W), during 1953–1987 [6] and at Tokyo, Japan (35.68° N, 139.77° E), during 1961–1979 [6]. At Ottawa, peak depositions of ^3H were observed in 1954, 1958, and 1963, and at Tokyo, a ^3H peak in precipitation was observed in 1963 [6]. The peaks in 1963 were caused by intensive atmospheric thermonuclear testing by the United States (conducted at 12° N) and the Soviet Union (at 73° N) in 1962. Although Ottawa and Tokyo are at middle latitudes in the northern hemisphere, the depositional delay of less than one year between the injection of ^3H into the stratosphere and its deposition in precipitation at those sites is too short. We nevertheless assumed that ^3H began to infiltrate downward from the ground surface at the borehole site (40.95° N, 141.56° E) in 1963.

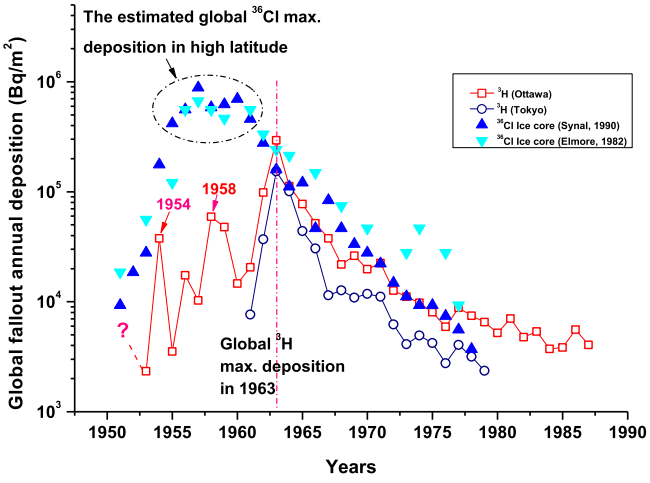


Fig. 3. Comparison of the global activated fallouts of ^{36}Cl in Ice core and ^3H in precipitation, Northern hemisphere.

Although the ^{36}Cl concentration in precipitation in the early 1960 s was not measured in Japan or elsewhere in the world, we reconstructed the Arctic ^{36}Cl deposition rate from the ^{36}Cl concentration in the Dye-3 (65.11° N, 43.50° W) Greenland ice core [15,16] (Fig. 3). Zerle et al. [17] estimated that large amounts of ^{36}Cl were injected into the stratosphere in 1954, 1956, and 1958 by large nuclear tests conducted on barges in the equatorial Pacific Ocean, with the largest amount injected in 1954. Phillips [2] inferred that the maximum ^{36}Cl concentration measured in the Dye-3 ice cores in 1957 reflected ^{36}Cl injected into the stratosphere in 1954, a delay of three years [16]. Furthermore, Zerle et al. [17] studied the concentration profile of aerosol-bound ^{137}Cs in glacial ice in Switzerland and suggested that gaseous ^{36}Cl was deposited at middle latitude sites (40–50° N) after a one-year delay. On the basis of the large deposition of gaseous ^3H observed in precipitation at Ottawa in 1954, we can infer that a large amount of similarly gaseous ^{36}Cl was deposited during 1954–1957 at the borehole site, with a maximum error of three years.

Therefore, we concluded that the maximum deposition of ^{36}Cl global fallout occurred from 1954 to 1957, and that maximum deposition of ^3H global fallout was in 1963.

4.3. Profiles of dissolved ^4He concentration and excess ^3He

The total dissolved ^4He concentration ranged from 6.8×10^{-8} ccSTP/g at −50.00 m to 7.6×10^{-8} ccSTP/g at −175.00 m, except the porewater sample from −101.0 to −101.05 m in which the concentration was 1.7×10^{-7} ccSTP/g (Fig. 4). These values are almost in equilibrium with the atmospheric ^4He concentration. In the groundwater sample from −257.00 to −262.00 m (close to the sandstone-mudstone boundary) and in the porewater sample from −377.00 to

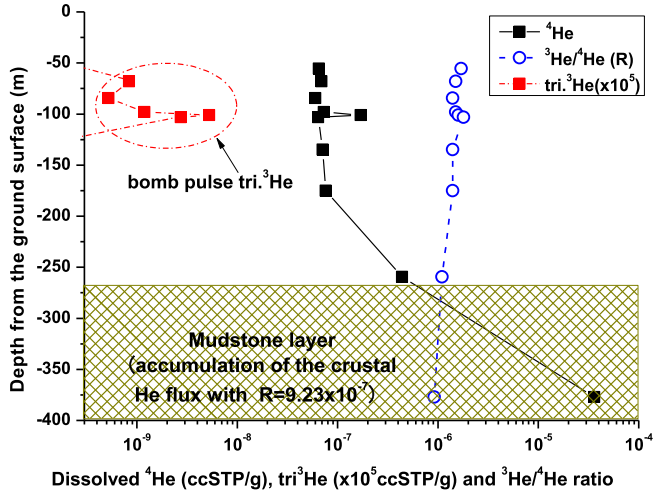


Fig. 4. Profiles of ^{4}He concentration, $^{3}He/^{4}He(R)$ ratio and the estimated tri.^{3}He concentration in the new borehole (depth of the bomb pulse peak: GL.-101 m deep).

−377.05 m (within the low-permeability mudstone), the dissolved ^{4}He concentration increased sharply from 4.4×10^{-7} to 3.6×10^{-5} ccSTP/g. In contrast, the $^{3}He/^{4}He$ ratio in both groundwater and porewater samples decreased monotonically from 1.7×10^{-6} to 9.3×10^{-7} with increasing sample depth, except between −97.95 and −103.05 m, where it increased slightly. Both the increasing dissolved ^{4}He concentration and the decreasing $^{3}He/^{4}He$ ratio result from addition of tri^{3}He and/or a local crustal He component, according to our previous study [1]. Crustal He ($^{3}He/^{4}He = 9.23 \times 10^{-7}$ measured in the core sample collected at −377.03 m) was found to represent a mixture of 91.5% radiogenic He (the maximum $^{3}He/^{4}He$ ratio was estimated to be 9.5×10^{-9} from the U, Th, and Li contents in mudstone [1]) and 8.5% mantle He ($^{3}He/^{4}He = 1.1 \times 10^{-5}$ in the subduction zone [18]). However, the anomalous variation in the $^{3}He/^{4}He$ ratio in the −97.95 to −103.05 m interval reflects the addition of He with a higher $^{3}He/^{4}He$ ratio (2.3×10^{-6} or more) than the local crustal value. Some amount of tri^{3}He was probably added in the interval from −69.7 to −103.03 m, but no additional tri^{3}He was estimated for the interval from −134.9 m to −377.03 m (Table 1). Furthermore, according to the results of three-dimensional analyses of groundwater flow and dissolved He transport [1], groundwater flows downward to the bottom of the basin below the tableland, except at the basin margin, where there is a shallow brackish marsh. The deep groundwater flow was very slow below −250 m and at −450 m in the mudstone layer, close to the basin floor, it was almost stagnant (less than 10^{-4} m/y). Therefore, upward dispersion of ^{3}He from crustal He was limited to vicinity of the mudstone layer boundary at −268 m. The anomalously high $^{3}He/^{4}He$ from −97.98 to −103.03 m thus indicates that tri^{3}He was added by β-decay of ^{3}H in rainwater that began to infiltrate downward from the ground surface in 1963 (see Table 1 and Fig. 4).

Consequently, the global fallout peak of ^{3}H in 1963 had arrived at around –101.00 m by the sampling date in 2001. The large excess ^{3}He concentration in groundwater and porewater below −257.00 m is attributable to the long-term accumulation of ^{3}He derived from the crustal He component supplied from the deep massive mudstone layer and implies that the residence time of the groundwater in the mudstone is very long.

4.4. Cl^{-}, $^{36}Cl/Cl$, and ^{36}Cl profiles in groundwater

In groundwater samples from the borehole, the Cl^{-} concentration profile varied irregularly between 15 and 40 mg/L in the interval from −53.0 to −220.0 m, and then increased from 140 to 17,000 mg/L from −257.0 to −376.0 m. The $^{36}Cl/Cl$ ratio was $(6.8 \pm 2.6) \times 10^{-15}$ from −53.0 to −58.0 m, reached a maximum of $(80.6 \pm 5.5) \times 10^{-15}$ from −132.0 to −145.0 m, and then decreased to $(4.3 \pm 1.8) \times 10^{-15}$ at −376.0 to −387.0 m. The number of ^{36}Cl atoms per liter of groundwater increased sharply from −132.0 m to a peak of 3.01×10^{7} atoms/L at −145.0 m, despite the dissolved Cl^{-} concentration being almost constant in that interval; it then sharply decreased downward to −220 m. Below that, it again increased, reaching 3.23×10^{7} atoms/L at −257 m, and the maximum concentration of 1.24×10^{9} atoms/L was reached at −376.0 m (Fig. 5).

We inferred that the ^{36}Cl peak from −132.0 m to −145.0 m represented the bomb pulse of global ^{36}Cl fallout, not only because the number of ^{36}Cl atoms (3.01×10^{7} atoms/L) in this peak was the highest in the interval from −53.0 m to −220.0 m but also because the maximum $^{36}Cl/Cl$ ratio was also reached at this depth. Below the mudstone layer boundary, the number of ^{36}Cl atoms per liter increased with increasing groundwater salinity; conversely, the $^{36}Cl/Cl$ ratio decreased with increasing salinity to $4.3 \pm 1.8 \times 10^{-15}$. In the mudstone layer, ^{36}Cl atoms probably accumulated as the result of in situ neutron absorption by ^{35}Cl, which has a relatively large neutron absorptive cross section (43.6 barn). By our previously described method [21,22], we estimated the secular equilibrium ratio of brine in the mudstone during the Miocene to late Pleistocene collected at the site to be 6.74×10^{-15} (Table 2). The residence time of the brine ($4.4 \pm 1.4 \times 10^{5}$ years) inferred from the calculated secular $^{36}Cl/Cl$ ratio is in line with the He

Table 1
Tritiogenic ^{3}He (tri^{3}He) concentrations in rock porewater samples, estimated by the model (tri)^{3}He = total ^{3}He – (sat)^{3}He – (e.a)^{3}He – (a.c.He)^{3}He [19]

Depth (GL. m)	total ^{4}He (ccSTP/g)	$^{3}He/^{4}He$	Ne (ccSTP/g)	total ^{3}He (ccSTP/g)	(sat)^{3}He[a] (ccSTP/g)	(e.a.)^{3}He[b] (ccSTP/g)	(a.c.He) ^{3}He[c] (ccSTP/g)	(tri)^{3}He[d] (ccSTP/g)
−55.50	6.50E−08	1.70E−06	2.90E−07	1.11E−13	6.47E−14	3.39E−14	N. E.[e]	N. E.
−67.90	6.90E−08	1.50E−06	2.80E−07	1.04E−13	6.47E−14	2.98E−14	6.50E−16	8.34E−15
−84.35	6.00E−08	1.40E−06	2.20E−07	8.40E−14	6.47E−14	5.64E−15	8.47E−15	5.22E−15
−97.98	7.30E−08	1.50E−06	2.70E−07	1.10E−13	6.47E−14	2.58E−14	7.15E−15	1.19E−14
−101.03	1.70E−07	1.60E−06	5.00E−07	2.72E−13	6.47E−14	1.19E−13	3.62E−14	5.26E−14
−103.03	6.40E−08	1.80E−06	2.60E−07	1.15E−13	6.47E−14	2.18E−14	1.37E−15	2.74E−14
−134.90	7.10E−08	1.40E−06	3.60E−07	9.94E−14	6.47E−14	6.21E−14	N. E.	N. E.
−174.98	7.60E−08	1.40E−06	3.50E−07	1.06E−13	6.47E−14	5.81E−14	N. E.	N. E.
−259.50	4.40E−07	1.10E−06	6.00E−07	4.84E−13	6.47E−14	1.59E−13	2.64E−13	N. E.
−377.03	3.60E−05	9.20E−07	3.90E−07	3.31E−11	6.47E−14	7.42E−14	3.39E−11	N. E.

[a] We hypothesized that ^{3}He concentration in precipitation was recharged at the average temperature (8 °C) at the site. The estimation included the max. ± 4% error.
[b] ^{3}He concentration in excess air in the recharged precipitation at the site, estimated from the Ne concentration by using the model of Torgersen et al. [20].
[c] ^{3}He concentration supplied from crustal He (a mixture of mantle He and radiogenic ^{3}He accumulated in deep groundwater).
[d] Tritiogenic ^{3}He produced by β decay of tritium in groundwater.
[e] If the correction of the accumulating crustal ^{3}He by the model used in our previous study [1] resulted in a negative value, we did not evaluate.

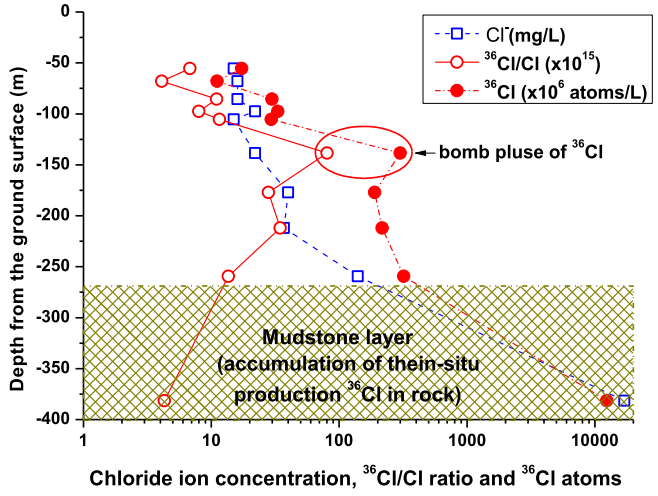


Fig. 5. Profiles of chloride concentration, $^{36}Cl/Cl$ (R) ratio and ^{36}Cl atoms/L in the new borehole (location of the bomb pulse peak: GL.-138 m deep).

dating results estimated from the He accumulation data [1]. As discussed in Section 4.3, from −220 m downward to the basin floor, the groundwater flow was basically downward and very slow; therefore, similar to ^{3}He, upward diffusive dispersion of in situ activated ^{36}Cl in the mudstone was limited to the vicinity of the mudstone boundary.

4.5. Estimation of downward groundwater flow velocity in the small tableland

The depth in the borehole of the ^{36}Cl bomb pulse differed substantially from that of the tri^{3}He bomb pulse because the timing of maximum global fallout deposition at the site differed between ^{36}Cl and ^{3}H (see Section 4.2). Because the maximum deposition of ^{3}H in precipitation was observed at both Tokyo and Ottawa in 1963 [6], the maximum ^{3}H deposition likely occurred at the same time on this small tableland. However, as we discussed in Section 4.2, intense deposition of ^{36}Cl probably occurred on the tableland during 1954–1957.

In 2001, the bomb pulse depth of tri^{3}He was at −101 m and that of ^{36}Cl was at −138 m. The assumption of piston flow from the ground surface to −220 m in the tableland is acceptable, because, as discussed

Table 2
Estimation of the neutron flux and secular ratio of $^{36}Cl/Cl$ in mudstone saturated with high-salinity water (17,000 ppm Cl^{-}).

Element (i)	E.C. (ppm)	M.S.P.[a]	W.F[b]	n/y/gi (U)[c]	n/y/g$_R$ U[d]	n/y/gi (Th)[c]	n/y/g$_R$ Th[d]	A. C-S[e]	At. W.[f]	Macro-ab[g]
C	187.2	561	0.11	0.45	0.05	0.18	0.02	3.53E−03	12.01	3.31E−02
N	93.6	550	0.05	1.92	0.10	1.10	0.06	7.47E−02	14.00	3.01E−01
B	1.9	527	0.00	62.08	0.06	19.67	0.02	7.64E+02	10.81	7.97E+01
Li	22.8	548	0.01	23.68	0.30	10.37	0.13	7.10E+01	6.94	1.40E+02
Cd	0.0							4.14E+03	112.41	1.04E+00
Gd	4.0							4.90E+04	157.25	7.47E+02
Eu	0.7							4.75E+03	151.97	1.30E+01
Be	0.3	529	0.00	265.95	0.04	90.87	0.01	7.60E−03	9.01	1.33E−04
F	355.8	472	0.17	40.97	6.88	16.19	2.72	9.57E−03	19.00	1.08E−01
Al	61466.7	444	27.55	5.05	137.90	2.55	69.57	2.31E−01	26.98	3.17E+02
Cl	3425.8	431	0.95	1.30	1.92	0.38	0.56	3.35E+01	35.45	1.95E+03
H	22631.9		0.00		0.00		0.00	3.33E−01	1.01	4.50E+03
O[l]	490716.9	527	255.85	0.24	61.03	0.08	21.72	2.80E−04	16.00	5.17E+00
Si	319502.4	454	146.44	0.68	98.64	0.33	48.45	1.77E−01	28.09	1.21E+03
Ca	1291.6	428	0.56	0.04	0.02	0.03	0.01	4.08E−01	40.08	7.91E+00
Mg	9055.1	461	4.21	5.77	24.09	2.53	10.58	5.03E−02	24.31	1.13E+01
Na	3945.2	456	1.80	12.40	22.30	5.87	10.57	5.31E−01	22.99	5.49E+01
K	24832.3	414	10.38	0.12	1.18	0.08	0.82	2.10E+00	39.10	8.02E+02
Fe	46238.6	351	16.39	0.18	2.95	0.20	3.29	2.59E+00	55.85	1.29E+03
Mn	4960.8	351	1.76	0.15	0.26	0.19	0.32	1.34E+01	54.94	7.29E+02
Ti	1935.9	383	0.75	0.87	0.65	0.52	0.39	6.10E+00	47.88	1.48E+02
P	322.9	433	0.14	0.86	0.12	0.57	0.08	1.70E−01	30.97	1.07E+00
S	11282.7	439	5.00	0.10	0.51	0.10	0.51	5.16E−01	32.07	1.09E+02
Sm	5.2							5.60E+03	150.40	1.17E+02
U	2.5								238.03	
Th	7.4								232.04	
Total U (ppm)	1000000 Sp-U[h]	a[i]	472.2977 Total U (n/g)/y[k]	358.21709 Th (ppm)	b[j]	169.4631 Total Th (n/g)/y[k]		Total (n/g)/y[k]	Neutron Flux (n/cm2/s)	1.22E+04 (μbarn) **Secular equilibrium ratio of $^{36}Cl/Cl$**
1	0.46	0.76	3.06	1	0.36	2.63		5.70	1.48E−05	**6.74E−15**

[a] Mass stopping power for α-particles (Mev/(g/cm^2) [23].
[b] Weight factor [24].
[c] Elemental neutron yields [25].
[d] Neutron yield per gram of rock per U concentration (ppm) and Th concentration (ppm); units (n/y/gRock).
[e] Thermal neutron absorption cross-section (10^{24} cm^2).
[f] Atomic weight.
[g] Macro-absorption thermal neutron cross section (10^{6} cm^2/g rock).
[h] Spontaneous fission neutron yield of 1 ppm U per gRock.
[i] Neutron yield of 1 ppm U per gRock from (α,n) reaction.
[j] Neutron yield of 1 ppm Th per gRock from (α,n) reaction.
[k] We used 0.44 as the effective porosity of an average rock in this calculation.
[l] O estimated from SiO_2 for Si, Al_2O_3 for Al, Fe_2O_3 for Fe, CaO for Ca, K_2O for K, Na_2O for Na, H estimated from porewater given the effective porosity of the rock, and Cl estimated from 17,000 ppm chloride ion dissolved in porewater.

in Sections 4.3 and 4.4, upward diffusive dispersion of crustal ^{3}He and in situ activated ^{36}Cl was probably not discernible at −220 m, which is approximately 50 m above the mudstone boundary. Moreover, downward transport of the radioactive tracers by advective flow together with diffusive dispersion would not change the position of the radioactive tracer's peak concentration, though the peak concentration would likely decrease. Because the dissolved concentrations of ^{4}He and chloride ions did not drastically vary (in fact, the concentrations of both these tracers were approximately constant to −220 m), it is reasonable to use a piston flow model without dispersive diffusion to estimate the downward groundwater velocity from the bomb pulse peak positions of the two tracers.

Under the assumption that groundwater moves vertically downward by piston flow at the site, the vertical flow velocity estimated from the depth of the tri^{3}He bomb pulse is 2.7 m/y, whereas that estimated from the depth of the ^{36}Cl bomb pulse ranges from 2.9 to 3.1 m/y. Thus, the estimated velocities differ by 10–15%. We attribute this difference mainly to the uncertainty in the estimated timing of the maximum deposition of global ^{36}Cl fallout at the site, though other effects such as differences in hydraulic conductivity of the rocks within the interval containing the ^{36}Cl and tri^{3}He bomb pulse peaks or differences in sampling section lengths might have contributed to the discrepancy. In addition, the fact that ^{36}Cl atoms dissolved in groundwater move faster than water molecules in saturated geological strata owing to repulsion between ^{36}Cl anions and the negatively charged surface of the surrounding rocks [26] may also account for the difference. More observational data for ^{36}Cl deposition and further tests and analyses are needed to assess the reason for the difference in the vertical flow velocities estimated from the depths of the tri^{3}He and ^{36}Cl bomb pulses.

5. Conclusions

1. In the study area, soil water and shallow and deep groundwater principally derive from meteoric water (i.e., rainwater), as indicated by the distributions of δD and δ^{18}O values. Moreover, stable isotopic variations can also be used to distinguish between summer (April–September) and winter (October–March) precipitation at the site.
2. The maximum deposition of the global ^{36}Cl fallout was inferred to have occurred during 1954–1957 and that of ^{3}H was inferred to have occurred in 1963, by considering the time lag between the injection of gaseous radionuclides into the stratosphere above nuclear weapons testing sites and their deposition at the study site.
3. The vertical downward flow velocity of groundwater in the tableland was roughly estimated by assuming piston flow and using the depths of the bomb pulse peaks of global ^{36}Cl and tri^{3}He fallout as time indicators. In this way, the groundwater velocity was estimated to be 2.7 m/y from the ^{3}H (i.e., tri^{3}He) bomb pulse depth and 2.9–3.1 m/y from the ^{36}Cl bomb pulse depth. The 10–15% difference in the estimates can be attributed mainly to the lack of observational data for ^{36}Cl deposition at the site.

Acknowledgements

We thank Prof. L. K. Fifield (Australian National University, Australia) for measuring ^{36}Cl in groundwater, and Dr. A. Saeki (retired from CRIEPI) for his contribution to this study. Further, we thank two anonymous reviewers for constructive comments and suggestions on the manuscript.

References

[1] Y. Mahara, T. Igarashi, Appl. Geochem. 18 (2003) 719.
[2] F.M. Phillips, Environmental Tracers in Subsurface Hydrology, Kluwer Academic Publishers, 2000, p. 299.
[3] J. Stone, J. Evans, K. Fifield, R.G. Cresswell, G. Allan, Radiocarbon. 38 (1996) 172.
[4] F.M. Phillips, Soil Sci. Soc. Amer. J. 58 (1994) 15.
[5] Y. Miyake, H. Matsuzaki, K. Sasa, T. Takahashi, Nucl. Instr. and Meth. B 361 (2015) 627.
[6] IAEA, Statistical treatment of data on environmental isotopes in precipitation. IAEA, Vienna. Tech. Rep. No. 331 (1992).
[7] H.L. Penman, Proc. R. Soc. London Ser. A. 193 (1948) 120.
[8] R.K. Schofield, Trans. Intern. Cong. Soil Sci. 3rd 2 (1935) 37.
[9] Y. Mahara, T. Ohta, T. Tokunaga, H. Matsuzaki, K. Nagao, E. Nakata, Y. Miyamoto, T. Kubota, Nucl. Instr. Meth. B 294 (2013) 597.
[10] D.C. Argento, J.O. Stone, L.K. Fifield, S.G. Tims, Nucl. Instr. Meth. B 268 (2010) 1226.
[11] Y. Mahara, Y. Ito, T. Nakamura, A. Kudo, Nucl. Instr. and Meth. B 223–224 (2004) 479.
[12] K. Nagao, M. Kusakabe, Y. Yoshida, G. Tanyileke, Geochem. J. 44 (2010).
[13] S. Waseda, N. Nakai, Geochem. J. 17 (1983) 83 (in Japanese).
[14] H. Craig, Science 133 (1963) 1702.
[15] D. Elmore, L.E. Tubbs, D. Newman, X.Z. Ma, R. Finkel, K. Nishiizumi, J. Beer, H. Oeschgar, M. Andrea, Nature 300 (1982) 735.
[16] H.-A. Synal, J. Beer, G. Bonami, M. Suter, W. Wölfli, Nucl. Instr. and Meth. B 52 (1990) 483.
[17] L. Zerle, T. Faestermann, K. Knie, G. Korschnek, E. Nolte, J. Geophys. Res. 102 (D16) (1997) 19517.
[18] Y. Sano, H. Wakita, J. Geophys. Res. 90 (1985) 8728.
[19] Y. Mahara, T. Ohta, N. Morikawa, T. Nakano, M. Tokumatsu, S. Hukutani, T. Tokunaga, T. Igarashi, Appl. Geochem. 50 (2014) 142.
[20] T. Torgersen, W.B. Clarke, W.J. Jenkins, Isotope hydrology Vol. 2 (1978) IAEA-SM-228/29.
[21] Y. Mahara, M.A. Habermehl, T. Haegawa, K. Nakata, T.R. Ransley, T. Hatano, Y. Mizuochi, H. Kobayashi, A. Ninomiya, B.R. Senior, H. Yasuda, T. Ohta, Earth Planet. Sci. Lett. 287 (2009) 43.
[22] Y. Mahara, T. Ohta, T. Tokunaga, H. Matsuzaki, E. Nakata, Y. Miyamoto, Y. Mizuochi, T. Tashiro, M. Ono, K. Nagao, Appl. Geochem. 27 (2012) 2389.
[23] J.F. Ziegler, The stopping and ranges of ions in matter vol. 4, Pergamon Press, New York, 1977.
[24] Y. Feige, B.G. Oltman, J. Kastner, J. Geophys. Res. 73 (1968) 3135.
[25] R. Heaton, H. Lee, P. Skensved, B.C. Robertson, Nucl. Geophys. 4 (1990) 499.
[26] E. Bresler, Soil Sci. Soc. Am. Proc. 37 (1973) 663.